J Mater Sci (2008) 43:2562–2573
DOI 10.1007/s10853-008-2472-x

Measuring the predictive accuracy of various models of formability of Corus Tubular Blanks

M. Evans

Received: 20 August 2007 / Accepted: 14 January 2008 / Published online: 20 February 2008

Abstract This paper assesses the predictive accuracy of various analytical models and one numerical model (a CART-ANFIS network) of springback that are available with the existing literature using the mean square error and its decomposition into systematic and random components as a comparative measure of predictive accuracy. The numerical model was found to have no systematic bias in the springback predictions made, whilst for the analytical models the systematic bias accounted for about 11% of the mean square error. The CART-ANFIS network also had the smallest MSE and the prediction errors made were all random in nature. The paper ends by giving some illustrations of the CART-ANFIS numerical model in finding the proper die contour to correct for springback so as to achieve right first-time manufacturing for a wide range of sheet steels.

Introduction

Government policy, consumer pressure and competition from materials such as aluminium and plastics have forced the automotive industry to search for methods of reducing the weight and improving the fuel economy of vehicles whose Body in White (BIW) predominantly comprises steel. Tube hydroforming and Laser Welded Tailor Blanks (LWTBs) are two relatively new innovations that help to reduce vehicle weight (see [1, 2]). The use of such advanced technologies, coupled with holistic design concepts, means that present-day vehicles are becoming lighter and have improved crash performance compared to conventional pressed formed components of the same weight.

Tube hydroforming has already proved successful in subframe and chassis applications. Standard tube-making methods are restricted to the production of tubes with a diameter-to-thickness ratio of 65:1, but BIW structural components typically require a ratio of around 100:1. There has therefore been limited uptake of this technology in the production of BIW components. However, the Corus Tubular Blank process [3, 4] enables a greater range of diameter-to-thickness ratios and therefore a larger scope for the manufacture of BIW parts. The Corus Tubular Blank Machine receives a flat sheet blank which undergoes a multiple pressing operation using a circular punch-and-die profile. The open formed tubular shape is then laser welded to form a closed section. The number of pressings required is dependent upon the degree of formability of the sheet blank and also the amount of forming pressure required to deform the sheet blank.

The major technical issue concerned with Corus Tubular Blanks is the effect of material elastic recovery (referred to as springback) after forming has taken place. The magnitude of this elastic recovery depends upon both material and forming properties. Whilst it is difficult to have full control over the material properties, forming properties are controllable, especially in the simple forming process of the Corus Tubular Blank. Thus the commonest method of compensating for springback is to bend the part to a smaller radius of curvature than is desired, so that when springback occurs, the component has the correct radius. This trial-and-error process can however be time consuming and expensive. Right first-time manufacturing of Corus Tubular Blanks can be achieved through use of an accurate predictive model of springback.

M. Evans (✉)
School of Engineering, Swansea University, Singleton Park, Swansea SA2 8PP, UK
e-mail: m.evans@swansea.ac.uk

The aim of this paper is to assess the accuracy of various analytical models and a numerical model of springback and then show how the best of these models can be used to find the proper die contour to correct for springback so as to achieve right first-time manufacturing for a wide range of sheet steels. To achieve this objective the paper is structured as follows. Section "Technical background" describes the Corus Tubular Blank Machine, how springback is measured and the experimental data obtained for assessing the accuracy of various springback models. Section "Predictive models of springback" outlines various analytical models and a numerical model for springback together with the methods of estimating the parameters of some of these models. Section "Predictive capability" describes some statistics for assessing the predictive accuracy of these models and the results from each of these models is given in section "Results". Section "Right first-time manufacturing" illustrates how the best model can be used for right first-time manufacturing and section "Conclusions" concludes.

Technical background

Bending and springback

Bending is the process by which a straight length is transformed into a curved length. The definitions of the terms used in bending are illustrated in Fig. 1a. The bend radius (R) is defined as the radius of curvature on the inside surface of the bend. For elastic bending below the elastic limit the strain passes through zero halfway through the thickness of the sheet at the neutral axis. In plastic bending—beyond the elastic limit—the neutral axis moves closer to the inside surface of the bend as such bending proceeds. Since the plastic strain is proportional to the distance from the neutral axis, fibres on the outer surface are strained more than fibres on the inner surface are contracted. A fibre at the mid-thickness is therefore stretched so that thickness decreases at the bend to preserve constant volume. The smaller the radius of curvature, the greater will be the decrease in thickness on bending.

A common forming difficulty during bending is springback. Springback is the dimensional change of the formed part after the pressure of the forming tool has been released. It results from the changes in strain produced by elastic recovery. This springback during bending is illustrated in Fig. 1b. This elastic recovery and therefore springback will be greater, the higher the yield stress and the lower the elastic modulus. The radius of curvature before release of a given load (R_0) is smaller than the radius (R_f) after release of this load. But the bend allowance (B in Fig. 1a) is the same before and after bending so that

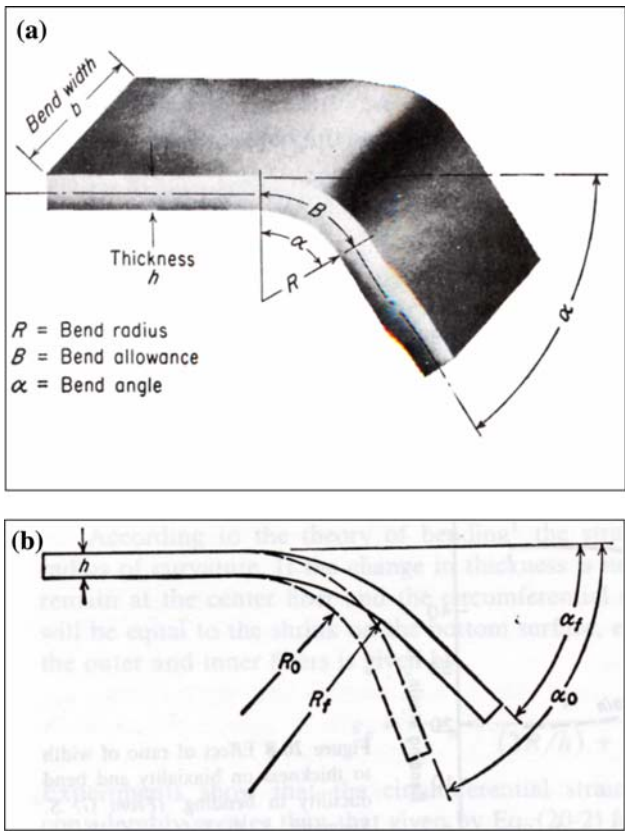

Fig. 1 (**a**) Definition of terms used in bending. (**b**) Springback in bending

$$B = \left(R_0 + \frac{h}{2}\right)\alpha_0 = \left(R_f + \frac{h}{2}\right)\alpha_f \tag{1a}$$

where h is the material thickness and α the bend angles (see Fig. 1b). This applies only if the mid-surface is also the neutral axis. Springback can be defined and measured from this in a number of ways. Defined in terms of the bend angle, the springback ratio is

$$K_1 = \frac{\alpha_f}{\alpha_0} = \frac{R_0 + h/2}{R_f + h/2} = \frac{2R_0/h + 1}{2R_f/h + 1} \tag{1b}$$

The springback ratio defined in this way is independent of sheet thickness and depends only on the ratio of bend radius to sheet thickness. Defined in terms of the bend radius, the springback ratio is

$$K_2 = \frac{R_0}{R_f} \tag{1c}$$

In this paper springback is defined and measured using Eq. 1c.

The Corus Tailored Blank and test rig machine

The Corus Tailored Blank Machine was developed by Soudronic Manufacturing, with initial conceptual ideas

coming from the research and development centre at the then Hoogovens Strip Steel in Ijmuiden, Holland [5]. The basic principle of the machine is to receive a flat sheet blank, which is then pressed using a circular punch-and-die profile used in conjunction with a hydraulic press. The open formed tubular shape is then finally laser welded to form a closed section. Pressing of the sheet is done in an uneven number of steps, with the sheet extremities pressed first and the unformed sheet progressively pressed towards the centre of the blank until the final pressing is carried out in the centre of the blank—see Fig. 2a. The number of pressings required for the blank is dependent upon the degree of formability of the blank and also the amount of forming pressure required to create the blank. The machine is currently capable of creating tubes with diameters in the range of 60–250 mm, with a thickness in the range of 0.6–2.75 mm and a length in the range of 900–4,750 mm [6].

The test machine used for the experimentation carried out during this research was a modified INSTRON™ MTS 8580. It is a 300 kN servo-hydraulic machine having a single force measuring system provided by a load cell. The system incorporates force scale settings giving a single range of 0 −300 kN in tension and compression (standard calibration BS EN 10002-2), coupled with programmable input and output hardware/software (INSTRON™ Wave-maker)—see Fig. 2b. This made it possible to control all suitable inputs for the pressing and the data acquisition during the pressing operation.

The experimental pressing tools, which were used in conjunction with the above test rig, were made of machine tool steel and the surfaces in contact with the material samples were case hardened. Prior to pressing, the tooling was degreased using an ethanol solution and then wiped clean using lint-free cloth. This test machine can be fitted

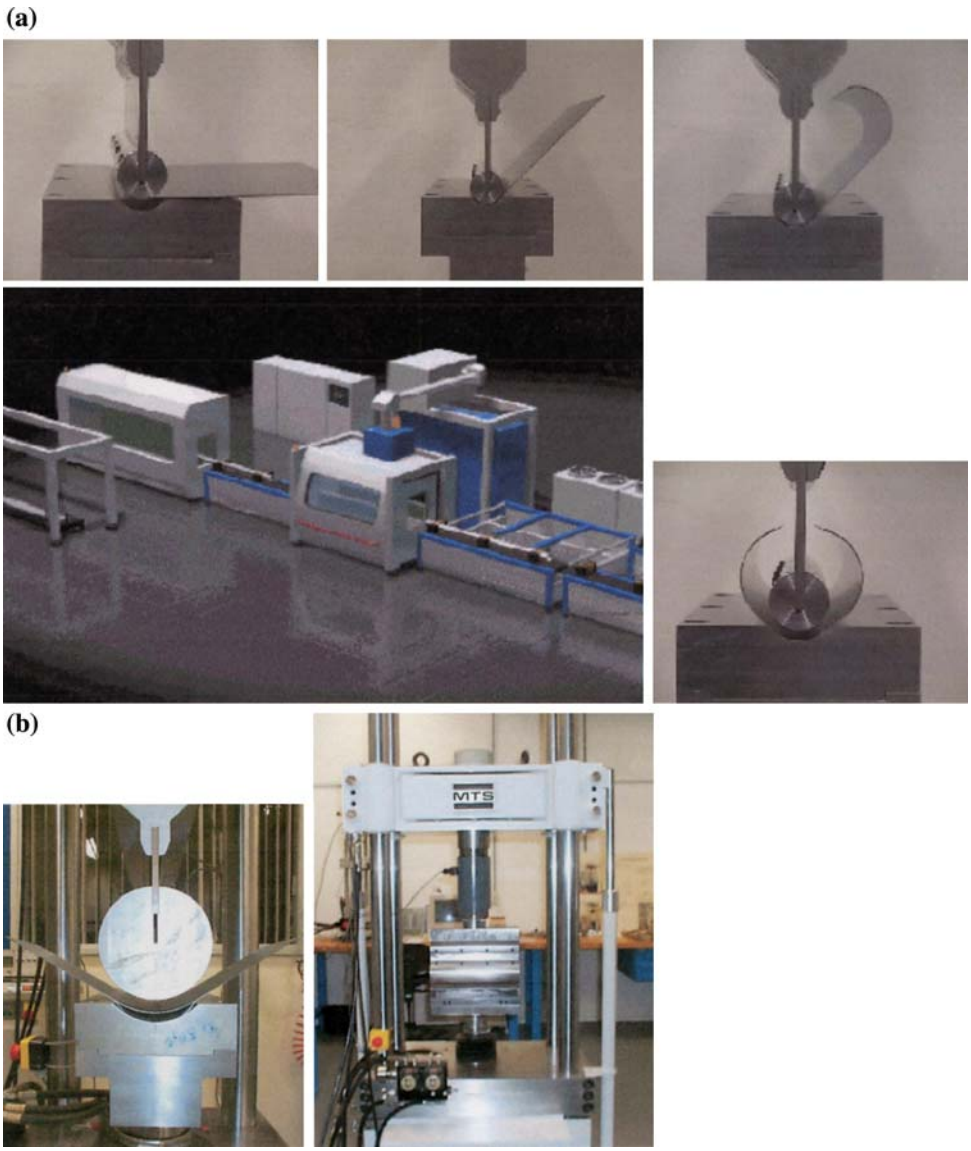

Fig. 2 (**a**) Corus Tubular Blank manufacturing route. (**b**) MTS testing machine and tooling used during experimentation

with a variety of different punch-and-die combinations, and the type of tooling fitted is similar to the tooling on the Corus Tailored Blank Machine shown in Fig. 2a.

The data

This MTS experimental tooling rig was used to test a variety of different steels that had differing material properties and thicknesses over a wide range of bend radiuses. The full test matrix, together with the springback measurements made under these conditions, is shown in Table 1. As can be seen from the first column of this table, the steels tested range from mild steels to CMn, IF and DP steels. The material properties tested included the yield stress (MPa) and Young's Modulus, whilst the process variables included material thickness and neutral axis bend radius (both measured in mm). These material and process variables, will be referred to later as test variables. For the purpose of data analysis, this paper scales all the test variables to lie in the range 0–1 through use of the formula

$$x_{j,i} = [x^*_{j,i} - \min(x^*_{j,i})]/[\max(x^*_{j,i}) - \min(x^*_{j,i})] \quad (1d)$$

where $x^*_{j,i}$ is the ith value (for which there are n) for the jth test variable (of which there are m), $\max(x^*_{j,i})$ is the maximum value for all n measurements made on test variable j and $\min(x^*_{j,i})$ is the minimum such value. As can be seen from Table 1, there are $n = 39$ steel specimens tested and $m = 4$ material or process conditions measured for each specimen. The same scaling procedure can be used for springback

$$y_i = [y^*_i - \min(y^*_i)]/[\max(y^*_i) - \min(y^*_i)] \quad (1e)$$

where y^*_i is the ith value for springback as measured using Eq. 1c.

Predictive models of springback

Analytical models

As briefly mentioned in section "Bending and Springback" above, springback will be greater, the higher the yield stress and the lower the elastic modulus. This has been expressed in the literature in a variety of different ways. Gardiner [7] and Queenner and DeAngelis [2], using data from a number of high temperature alloys, have indicated that to a first approximation the springback in bending can be expressed by

$$K_2 = 4\left(\frac{R_0\sigma_0}{Eh}\right)^3 - 3\frac{R_0\sigma_0}{Eh} + 1 \quad (2a)$$

where σ_0 is the plain strain yield stress and E is modified (plain strain value) Young's Modulus. Other approximations based on the same variables are also to be found in the literature. Marciniak and Duncan [8] proposed

$$K_2 = 1 - 3\left(\frac{R_0}{h}\right)\left(\frac{\sigma_0}{E}\right) \quad (2b)$$

Zhang and Hu [9] proposed a similar expression using Poisson's ratio. Leu [10] derived a slightly more complex equation that also took into account the ultimate tensile strength of the material and the normal plastic anisotropy ratio. This model for springback was derived from a number of simplifying assumptions. First, a ridged, strain-hardening and anisotropic material is assumed and the deformation in bending is assumed to occur under the plane strain condition. The Bauschinger effect and strain rate are neglected, and Hill's [11] theory of plastic anisotropic is adopted to describe the anisotropic characteristics of the sheet metal. Finally, the strain-hardening characteristics of the sheet metal are assumed to follow the form

$$\sigma_e = A\varepsilon_e^n \quad (2c)$$

where σ_e denotes the effective stress, ε_e denotes the effective strain and A and n are material constants. Under these conditions Leu showed that springback could be predicted using

$$K_2 = \left(\frac{\sigma_u}{e^{-n}n^n}\right)\left(\frac{1+r}{\sqrt{1+2r}}\right)^{1+n}\left(\frac{3(1-\nu^2)}{2E(1+n)}\right)\left(\frac{h}{2R_0}\right)^{n-1} \quad (2d)$$

where σ_u is ultimate tensile strength and r is the normal anisotropic value. Again n is the strain-hardening component as defined in Eq. 2c above.

The first two models above require no parameter estimation, whilst the last requires that the value for n be estimated from the experimental data.

Numerical models

There are many numerical procedures currently available for modelling experimental data obtained from a particular manufacturing process. The two most commonly used techniques are response surface methodology (RSM) and artificial intelligence (AI).

Response surface methodology is a well-established and proven collection of mathematical and statistical techniques useful for the modelling and analysis of manufacturing processes in which a response of interest is influenced by several variables and the objective is to optimise the response in some way [12]. The description of the bending process described above suggests that springback, to be given the general name response and symbol y, may be related to the following material and

Table 1 Springback results from the MTS experimental tooling rig

Material	i	1	2	$x^*_{1,i}$	$x^*_{2,i}$	$x^*_{3,i}$	$x^*_{4,i}$	$x^*_{5,i}$	y^*_i
Nizec 260	1	0	50	0.693	214,026	259	49.6535	389	0.701
GI IF240	2	0	50	0.653	206,901	242	49.6735	376	0.7098
DP 1300	3	90	7	0.996	187,000	1369	7.498	1489	0.7973
GA 260	4	90	43.5	0.991	214,000	312	43.0045	419	0.8146
DP 350	5	90	50	1.594	219,000	362	49.203	554	0.8167
CMn 500	6	90	50	2.001	213,000	555	48.9995	624	0.8175
GA 260	7	0	43.5	0.997	199,000	286	43.0015	417	0.8202
CMn 500	8	0	50	2.015	199,000	517	48.9925	610	0.8214
DP 350	9	0	50	1.532	208,000	361	49.234	547	0.8225
DP 350YP	10	90	50	1.49	215,000	403	49.255	443	0.832
GA 300	11	90	50	2.02	198,000	322	48.99	442	0.8444
GA 300	12	0	50	2.012	192,000	317	48.994	436	0.8444
DP 350YP	13	0	50	1.484	202,000	369	49.258	435	0.852
GA140	14	90	50	0.747	194,382	149	49.6265	305	0.8575
GA140	15	0	50	0.744	210,802	139	49.628	308	0.8627
GA 300	16	90	18.5	0.838	215,000	330	18.081	436	0.8629
DP 850	17	45	7	1.191	176,000	850	7.5955	1089	0.863
GA 300	18	0	18.5	0.787	204,000	322	18.1065	459	0.869
GA 260	19	90	18.5	0.813	229,000	274	18.0935	423	0.8754
GA 260	20	0	18.5	0.814	202,000	253	18.093	417	0.8793
GA 140	21	90	43.5	1.007	201,000	168	42.9965	305	0.884
DP 630	22	90	7	1.223	184,000	631	7.6115	836	0.8954
GA 200	23	90	50	2.07	194,000	207	48.965	332	0.8972
GA 200	24	0	50	2.047	184,000	201	48.9765	340	0.9
DP 400	25	45	7	1.191	188,000	405	7.5955	671	0.9271
GA 140	26	90	18.5	0.812	197,000	145	18.094	303	0.9309
DP 500	27	90	7	1.956	181,000	509	7.978	812	0.9315
GA 140	28	0	18.5	0.811	201,000	159	18.0945	307	0.9335
GI IF 240	29	0	7	0.653	206,901	242	7.3265	376	0.9402
CMn 700	30	90	7	2.545	176,000	699	8.2725	776	0.9434
DP 400	31	45	7	1.782	171,000	425	7.891	653	0.9485
DP 350YP	32	0	7	1.484	202,000	369	7.745	435	0.9617
GA 140	33	0	7	0.744	210,802	139	7.3735	308	0.968
Nizec 260	34	90	50	0.703	215,713	254	49.6485	385	0.6984
GA 180	35	90	7	0.688	191,000	185	7.344	311	0.9503
GA 140	36	0	43.5	1.005	184,000	161	42.9975	305	0.892
DP 800	37	0	7	0.998	196,000	836	7.4955	1076	0.8392
DP 350	38	0	7	2.025	172,000	371	8.0125	609	0.9621
GI IF240	39	90	50	0.653	212,187	261	49.6735	373	0.7047

1 = Orientation (°), 2 = Bend Radius (mm), $x^*_{1,i}$ = Thickness (mm), $x^*_{2,i}$ = Young's Modulus, $x^*_{3,i}$ = Yield Stress (MPa), $x^*_{4,i}$ = Neutral Axis Bend Radius (mm), $x^*_{5,i}$ = Ultimate Tensile Strength (MPa), y^*_i = Springback (as measured by K_2 in Eq. 1c)

process variables: x_1 is the sheet thickness, x_2 is Young's Modulus, x_3 is the yield strength and factor x_4 is the neutral axis bend radius (all in scaled units). Then the response surface is given by

$$y = f(x_1, x_2, x_3, x_4) \tag{3a}$$

where $f()$ is some function that describes the relationship existing between springback and the process and material variables described above. In most RSM problems the form of $f()$ is unknown and the first step is therefore to find a suitable approximation for the true functional relationship between y and the test variables. As many manufacturing

processes are non-linear in nature, Myers and Montgomery [13] recommend approximating $f()$ by a second-order response surface models of the form

$$f(x_1,x_2,x_3,x_4)=\beta_0+\beta_j\sum_{j=1}^{4}x_j+\lambda_{jv}\sum_{j=1}^{4}\sum_{v=j+1}^{4}x_jx_v+\phi_j\sum_{j=1}^{4}x_j^2+\omega \quad (3b)$$

where β_j, ϕ_j and λ_{jv} are the parameters of the model. The λ_{jv} measure interaction effects and reflect the extent to which a change in the response following a change in the level of a test variable depends partly on the value for another test variable. ω is the component of y that cannot be explained by the model. Provided that ω is a random variable, this model provides a reasonable approximation to the response surface. For all these models the parameters β_0, β_j, ϕ_j and λ_{jv} require estimation using the linear least squares estimation procedure.

Artificial intelligence is a big subject area covering numerous types of neural network architectures, genetic algorithms and expert or control systems. A relatively new and interesting approach that merges the subject areas of neural networks and control systems is the fuzzy—neural network. A popular neural network architecture is the multi-layer perceptron (MLP). However, whilst MLPs are usually better than the RSM at approximating the response surface, they are very much a black box technique in that they generate very complex functions that simply mimic the data accurately. What they cannot do is abstract in the sense of producing articulated knowledge from the data. Expert systems are capable of such abstraction through the use of simple rule-based models. Neuro-Fuzzy modelling is a new approach that combines the modelling capabilities of MLPs with the abstracting capabilities of expert systems. In this paper we concentrate on the hybrid technique CART-ANFIS that is capable of learning and then fine tuning hybrid rules.

Characterisation and Regression Trees (CART) is a technique first developed by Breiman et al. [14]. Here binary decision trees are used to extract simple if—then-based decision rules from the experimental data. Figure 3a is a typical binary regression tree with two inputs (x_1 and x_2) and one output y. The decision tree partitions the input space into a number of non-overlapping rectangular regions, each of which is assigned a label $f_i()$ to represent a predicted output value. In this illustration the tree identifies four simple if—then rules. Note that each terminal node has a unique path that starts with the root node and ends with the terminal node: the path corresponds to a decision rule that is a conjunction of various tests or conditions. Typically each $f_i()$ will be a linear function similar to the first two terms in Eq. 3b. In essence then, instead of using a complex second-order response surface model, the experimental data are split up into smaller segments such that over these narrower ranges the response surface is linear allowing the response to be modelled using a simpler linear equation over this region. For each region there is a separate linear equation.

The key question then revolves around the criteria for deciding how many terminal nodes to have in the decision tree, i.e., how many segments to split the data up into. In this paper two rules are used. First, there must be a minimum number of degrees of freedom available for fitting the $f_i()$ functions. In this paper that is taken to be five. Second, at each node a statistic is worked out for summarising how well $f_i()$ fits the data within its segment. Breiman et al. [14] used the standard residual sum of squares obtained by estimating the parameters of $f_i()$ using linear least squares. In this paper we use the predictive residuals of Cook and Weisburg [15]. Here the linear model $f_i()$ is estimated by least squares using all but one of the experimental data points in its segment. The difference between the actual value for this data point and that predicted from the model is the predicted residual. When this procedure is repeated for all data points the resulting sum of these predicted residuals is called the predicted residual sum of squares (PRESS). The estimated value for the parameters of $f_i()$ that minimise PRESS is the one best at predicting data not seen during this estimation procedure and so has the best chance of being general enough to accurately predict new data sets that are presented to it. That is, the linear models $f_i()$ are subjected to cross validation. A pair of terminal nodes on the decision tree are obtained when the values for their PRESS statistics sum to a figure that is no smaller than that associated with their root node.

Values for a, b and c in Fig. 3a are found by sorting each input variable. First the data set is sorted by x_1 from lowest to highest. The value for x_1 in the $p + 5$ position of this sorted list is taken to be the first estimate for a (p is the number of parameters to be estimated in the $f_i()$ function). The data are split at a and the PRESS statistics computed for each data segment. These are added together to give the total PRESS. The value for x_1 in the $p + 5 + 1$ position of this sorted list is taken to be the next estimate for a. This process is repeated until all the x_1 values in the sorted list have been analysed in the above way. The value for a is then taken to be that value which minimises the total PRESS statistic. Values for b and c are found in the same way after the value for a has first been decided.

The problem with this approach is that the resulting modelled response surface is highly discontinuous in that it changes abruptly at the decision rules. This problem is overcome by fuzzyfying the decision rules. For example, the crisp decision rule associated with the leftmost branch of the binary tree in Fig. 3a is

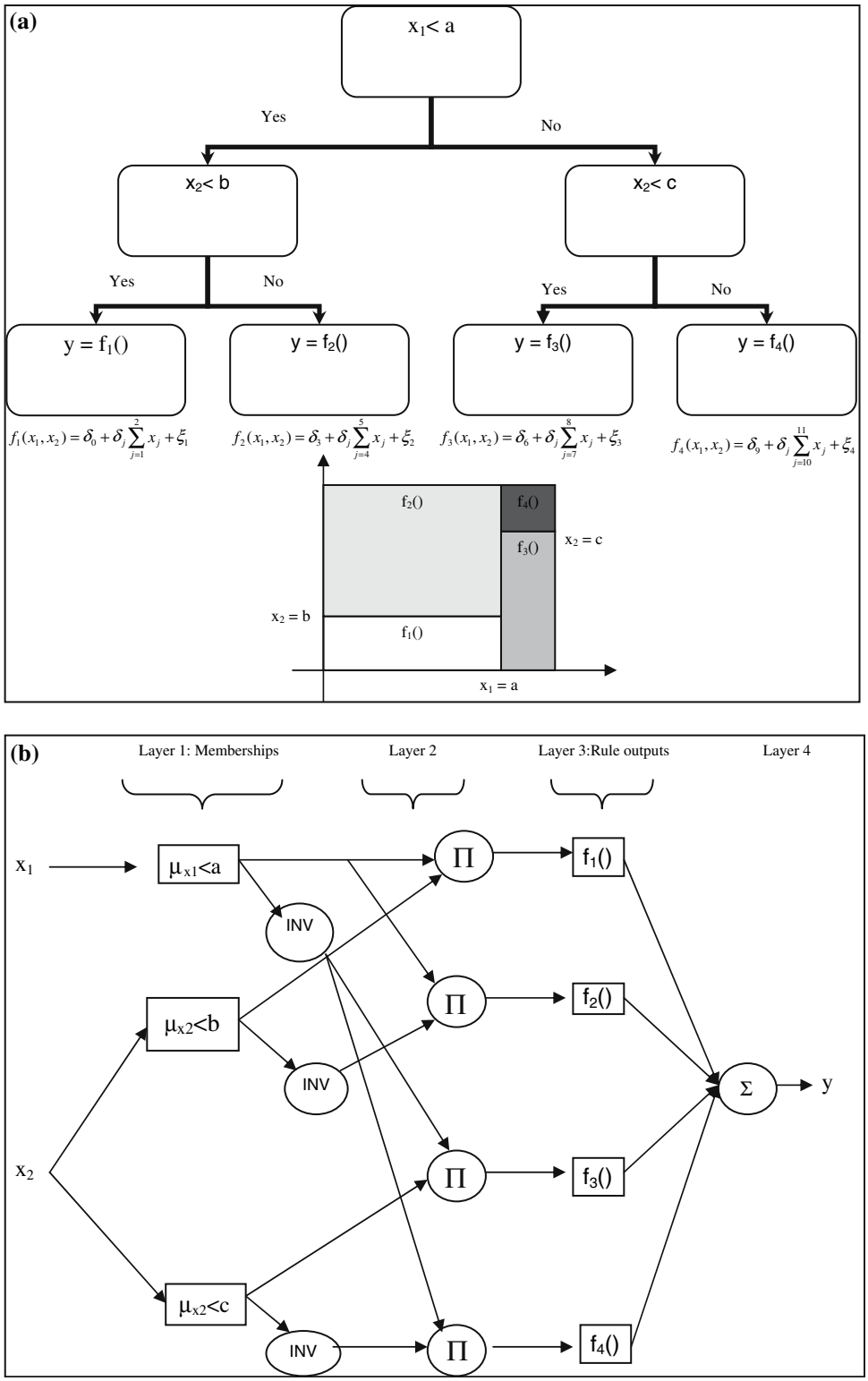

Fig. 3 (**a**) A binary decision tree and its input space partitioning. (**b**) ANFIS architecture corresponding to the representation shown in Fig. 3b. Values for *w* given by Eqs. 5

If $x_1 < a$ and $x_2 < b$ then $y = f_1()$

In fuzzy expert systems, membership functions are used to quantify possibilities [16]. Possibility is a fuzzy measure indicating the degree of evidence or belief that a certain value for say x_1 belongs to a set, say, set $x_1 < a$. A membership function has a value between 0 and 1 such that x_1 values further and further below a, have membership values closer and closer to one. A common functional form used for the membership function is the sigmoidal function

$$\mu_{x_1<a} = 1 - \frac{1}{1+\exp[-\kappa(x_1-a)]} \tag{4a}$$

where κ is a parameter requiring estimation. The value for κ determines the steepness of the membership function at a. So the further x_1 is below a, the greater will be the value for $\mu_{x_1<a}$, indicating a stronger belief that that value for x_1 belongs to the set $x_1 < a$. $\mu_{x_1<a}$ varies over the range 0–1, with 1 indicating the strongest possible belief.

Finally, the parameters of the model are fined tuned using a particular type of neural network. This network is called an ANFIS—adaptive network-based fuzzy interference system [17]. There are various ANFIS architectures, but the one using a first-order Sugeno fuzzy model [18] is the most common. The layers of this ANFIS network are shown in Fig. 3b for the decision rules shown in Fig. 3a

Rule 1: If $x_1 < a$ and $x_2 < b$, then $y = f_1()$
Rule 2: If $x_1 < a$ and $x_2 \geq b$, then $y = f_2()$
Rule 3: If $x_1 \geq a$ and $x_2 < c$, then $y = f_3()$
Rule 4: If $x_1 \geq a$ and $x_2 \geq c$, then $y = f_4()$

In the first layer of the ANFIS network, each of the i values for x_1 and x_2 is given membership quantities using the following sigmoidal functions

$$\mu_{x_1<a} = 1 - \frac{1}{1+\exp[-\kappa_1(x_1-a)]} \text{ with inverse (INV)}$$
$$\mu_{x_1\geq a} = \frac{1}{1+\exp[-\kappa_1(x_1-a)]} \tag{4b}$$

$$\mu_{x_2<b} = 1 - \frac{1}{1+\exp[-\kappa_2(x_1-b)]} \text{ with inverse (INV)}$$
$$\mu_{x_2\geq b} = \frac{1}{1+\exp[-\kappa_2(x_1-b)]} \tag{4c}$$

$$\mu_{x_2<c} = 1 - \frac{1}{1+\exp[-\kappa_3(x_1-c)]} \text{ with inverse (INV)}$$
$$\mu_{x_2\geq c} = \frac{1}{1+\exp[-\kappa_3(x_1-c)]} \tag{4d}$$

where κ_1 to κ_3 are parameters requiring estimation. In layer 2 weights are determined that represent the possibility that each pairing for the i values of x_1 and x_2 belongs to one of the four sets given by the decision rules above. These weights are given by

$$w_1 = (\mu x_1 < a)(\mu x_2 < b) \text{ or } w_1 = \min[(\mu x_1 < a), (\mu x_2 < b)] \tag{5a}$$

$$w_2 = (\mu x_1 < a)(\mu x_2 \geq b) \text{ or } w_2 = \min[(\mu x_1 < a), (\mu x_2 \geq b)] \tag{5b}$$

$$w_3 = (\mu x_1 \geq a)(\mu x_2 < c) \text{ or } w_3 = \min(\mu x_1 \geq a), (\mu x_2 < c)] \tag{5c}$$

$$w_4 = (\mu x_1 \geq a)(\mu x_2 \geq c) \text{ or } w_4 = \min(\mu x_1 \geq a), (\mu x_2 \geq c)] \tag{5d}$$

These are two examples of a T-norm operator (the product or the minimum) for working out the possibility, for example that x_1 is less than a AND x_2 is less than $b(w_1)$. In Fig. 3b, Π stands for the use of the first T-Norm shown in Eqs. 5. In layer 3 each value for $f_i()$ is multiplied by its w_i value so that more emphasis is placed on the linear function corresponding to the rule most likely to describe the x_1 and x_2 pairing (the form for $f_i()$ is as shown in Fig. 3a). Finally, in layer 4 these weighted functions are added up to give the prediction for y coming out of the ANFIS network. Conjugate gradient methods are then used to optimise the values for κ_1 to κ_3 and all the parameters of $f_1()$ to $f_4()$.

Predictive capability

A number of statistics are used to assess the predictive accuracy of the above springback models. The mean square error (MSE) is defined as the average (over n results) squared difference between the actual springback value (y_i) and that predicted by a particular model ($\hat{y}_i$). Squares are taken to prevent over- and under-predictions offsetting each other in the averaging process. The MSE could then be square rooted to be in the same units as y_i

$$\text{MSE} = \frac{1}{n}\sum_{i=1}^{n}[y_i - \hat{y}_i]^2 = \frac{1}{n}\sum_{i=1}^{n} e_i^2 \tag{6a}$$

Thus if the model used is that given by Eq. 3b, the predicted values are given by

$$\hat{y}_i = \beta_0 + \beta_j\sum_{j=1}^{4} x_j + \lambda_{jv}\sum_{j=1}^{4}\sum_{v=j+1}^{4} x_j x_v + \phi_j\sum_{j=1}^{4} x_j^2$$

where β_j, ϕ_j and λ_{jv} are estimated from the n data points. The MSE is a useful way of assessing the predictive accuracy of a model because this error, following Theil's analysis [19], can be decomposed into a number of different components

$$\text{MSE} = \bar{e}^2 + S_e^2 \tag{6b}$$

where $\bar{e}$ is the average prediction error calculated from the n data points and S_e^2 is the sample variance of the prediction error (biased in small samples). A good model will therefore predict with an average error close to zero and with only small over-/under-predictions around this average, i.e., small variation in the prediction error.

A plot of actual versus predicted springback values can be used to further decompose this MSE. On such a plot, all the data points should fall on a 45° line if the springback

model provides a perfect prediction. That is $\rho = 0$, $\rho_1 = 1$ and $S_\zeta^2 = 0$ in

$$y_i = \rho_0 + \rho_1 \hat{y}_i + \zeta_i \tag{7a}$$

where ζ_j is the extent to which the ith springback prediction differs from $\rho_0 + \rho_1 \hat{y}_i$ and S_ζ^2 is the variance of such disturbances. Rearranging Eq. 7a above for the prediction error and assuming $\hat{y}_i$ and ζ_i are independent of each other gives

$$S_e^2 = (\rho_1 - 1)^2 S_{\hat{y}}^2 + S_\zeta^2 \tag{7b}$$

where $S_{\hat{y}}^2$ is the variance of the predictions. Substituting Eq. 7b into Eq. 6b gives

$$\text{MSE} = \bar{e}^2 + \left\{(\rho_1 - 1)^2 S_{\hat{y}}^2\right\} + S_\zeta^2 \tag{8a}$$

or

$$1 = \frac{\bar{e}^2}{\text{MSE}} + \frac{\left\{(\rho_1 - 1)^2 S_{\hat{y}}^2\right\}}{\text{MSE}} + \frac{S_\zeta^2}{\text{MSE}} = U_M + U_R + U_D \tag{8b}$$

Equation 8b shows that a proportion of the MSE is due to the average of the model predictions differing from the average of the actual values —U_M. Another part is due to the slope of the best fit line on the actual v prediction plot differing from 1, U_R. Both U_M and U_R therefore represent systematic errors, and large values for these two terms suggest that the springback model is incomplete in some way. For example, it may suggest that some explanatory variables are missing from the model, or that the models functional relationship between springback and the test condition is incorrect. A final part of the MSE is due to the data points on the actual v prediction plot not all lying on the best fit line, U_D. When they all lie on the best fit line $S_\zeta^2 = 0$. As the ζ_i is random in nature, U_D represents random prediction errors. Ideally, a springback model should have a very small MSE with $U_M = U_R = 0$ and $1 \cong U_D$.

Results

Figure 4 plots the measured springback results against material thickness, Young's Modulus, yield stress and neutral axis bend radius. It can be seen that the data have a lot of experimental scatter present within it. However, the strongest correlations are observed to be those between springback and Young's Modulus ($R^2 = 24.45\%$), and between springback and the neutral axis bend radius ($R^2 = 42.23\%$). Material thickness and yield strength appear to have a much smaller impact on springback. However these are linear correlation coefficients, and the true relationships between these variables may be non-linear in nature so that the above interpretations may be misleading.

The predictive accuracy of various analytical models is summarised in Fig. 5 and Table 2. Figure 5a and b shows clearly that both analytical models produce fairly reasonable predictions. The best fit lines through the experimental data reveal a small amount of systematic bias with the intercept terms differing slightly from zero and the slope terms differing slightly more from unity. This is confirmed in Table 2. All these models have very similar mean square errors. For each model around 88% of the prediction errors were random in nature, and the main source of systematic error for each model was the deviation of ρ_1 in Eq. 7a from unity (i.e., U_R rather than U_M).

Table 3 shows the results of the CART analysis. As can be seen from the Table, the procedure described in section

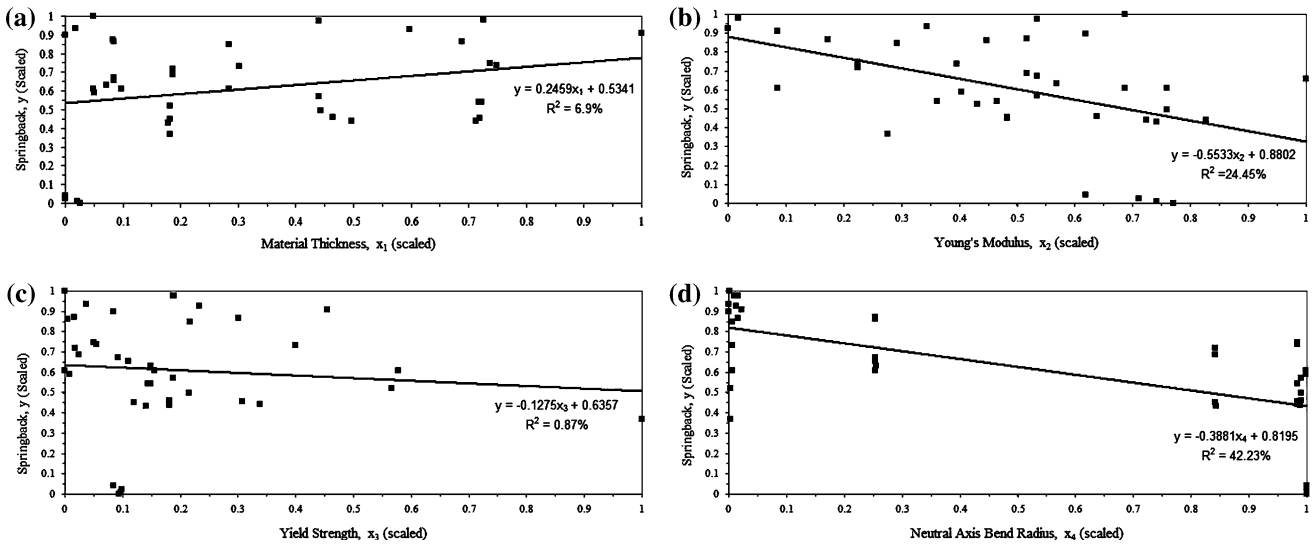

Fig. 4 Springback as a function of (**a**) Material thickness, (**b**) Young's Modulus, (**c**) Yield Strength and (**d**) Neutral axis bend radius

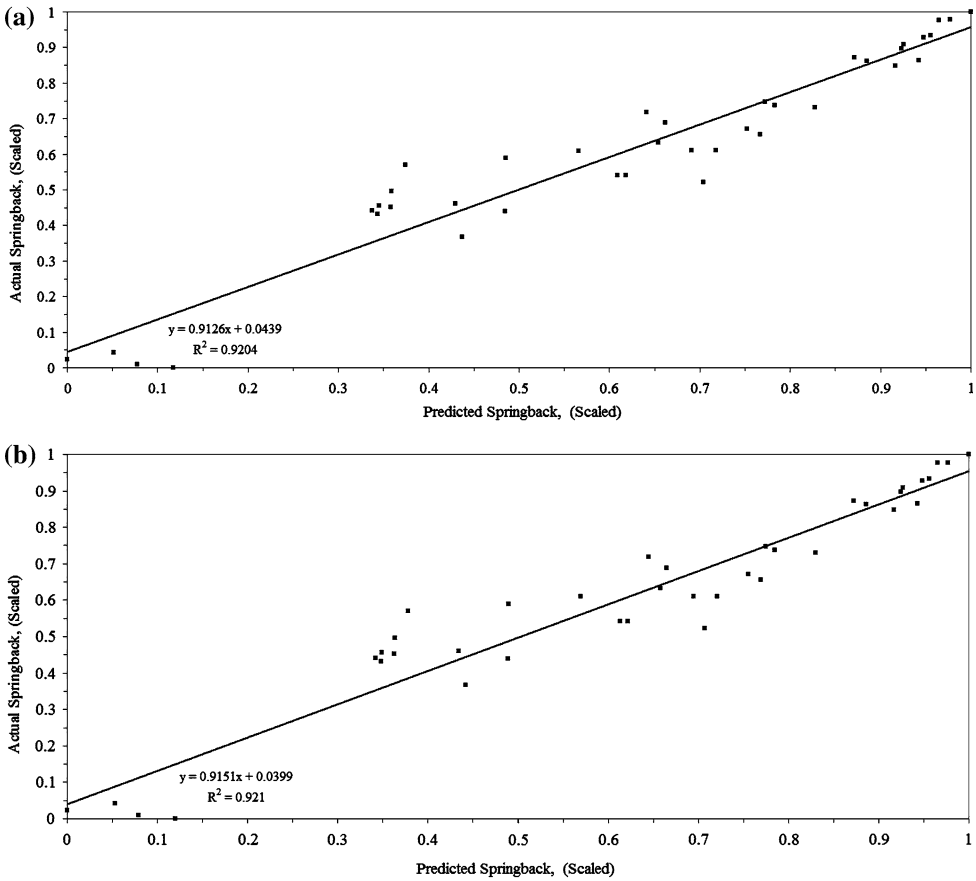

Fig. 5 (**a**) Actual versus predicted springback using the analytical technique proposed by Gardiner [7] and Queenner and DeAngelis [2]. (**b**) Actual versus predicted springback using the analytical technique proposed by Marciniak and Duncan [8] and Zhang and Hu [9]

Table 2 The MSE and its decomposition for various analytical springback models

	Gardiner [7] and Queenner and DeAngelis [2]	Marciniak and Duncan [8] and Zhang and Hu [9]
MSE	0.00639	0.00637
U_M	1.73	2.71
U_R	9.43	8.87
U_D	88.84	88.42

MSE is the mean squared error as defined by Eq. 6a. U_M, U_R, and U_D are % decompositions of the MSE as defined by Eq. 8b

"Numerical models" above identified three basic splits in the data corresponding to all those data points with a scaled yield stress less than or equal to 0.0992, all those data points with a scaled yield stress greater than 0.0992 but with a scaled thickness less than or equal to 0.4424 and all those data points with a yield stress greater than 0.0092 and a scaled thickness greater than 0.4424. Table 3 shows the estimates made for the parameters of the simple linear numerical model (containing the first two terms of Eq. 3b) that was applied separately to each of these subsets of data. In each subset, Young's Modulus was always statistically insignificant. This conclusion probably comes about because the data set is only for steel, and the modulus in the experiments shown in Table 1 varied only over the narrow range of 120—220 GPa. The worst performing linear model was that fitted to the first subset of data ($x_{3i} \leq 0.0992$) where the model $f_1()$ explained nearly 93% of the variation in springback. The percentage rose to around 97% in the second subset of data and around 99% in the third subset of data. This picture is confirmed also by the PRESS statistics.

Finally, the CART model was fuzzified by integrating it into an ANFIS network. This CART-ANFIS network predicts springback through the following estimated equations

$$y_i = w_{1,i} f_{1,i}() + w_{2,i} f_{2,i}() + w_{3,i} f_{3,i}() \tag{9a}$$

where

$$\begin{aligned} f_{1,i}() &= 1.31269 - 0.9448x_{1,i} - 1.8933x_{2,i} - 9.7294x_{3,i} \\ &\quad + 0.1962x_{4,i} \\ f_{2,i}() &= 1.3623 + 5.5162x_{1,i} + 2.7888x_{2,i} - 4.5244x_{3,i} \\ &\quad - 2.2389x_{4,i} \\ f_{3,i}() &= 0.3549 - 1.2928x_{1,i} - 1.3456x_{2,i} + 5.4331x_{3,i} \\ &\quad + 0.5992x_{4,i} \end{aligned} \tag{9b}$$

and

Table 3 Results of CART analysis

Parameter/Variable	If $x_{3i} \leq 0.0992$ then $f_1()$ =	If $x_{3i} > 0.0992$ and $x_{1i} \leq 0.4424$ then $f_2()$ =	If $x_{3i} > 0.0992$ and $x_{1i} > 0.4424$ then $f_3()$ =
β_0/Intercept	1.22192 (11.08*)	0.74721 (16.45*)	0.88966 (21.90*)
β_1/x_1	0.54143 (3.75*)	0.72219 (9.31*)	0.23620 (3.07*)
β_2/x_2	−0.25548 (−1.26)	0.00545 (0.11)	−0.079829 (−1.27)
β_3/x_3	−4.15477 (−5.61*)	−0.54865 (−11.82*)	−0.45902 (−4.12*)
β_4/x_4	−0.58325 (−8.94*)	−0.43172 (−15.28*)	−0.42052 (−11.74*)
R^2	92.50%	96.65%	99.41%
R^2_{PRESS}	88.27%	89.35%	98.93%
σ	0.09797	0.03111	0.01780
PRESS	0.22522	0.03695	0.00517

All parameters were estimated using linear least squares. The Student t statistics for testing the null hypothesis that the true parameters are equal to zero are shown in brackets

* t statistic rejects the null hypothesis at the 10% significance level. R^2 is the coefficient of determination adjusted for degrees of freedom calculated from the least squares residuals. R^2_{PRESS} is the coefficient of determination adjusted for degrees of freedom calculated from the predictive residuals. σ is the standard error of the least squares residuals and PRESS is the sum of the squares of the predictive residuals. Values for x_{ji} are scaled values derived from Eq. 1d

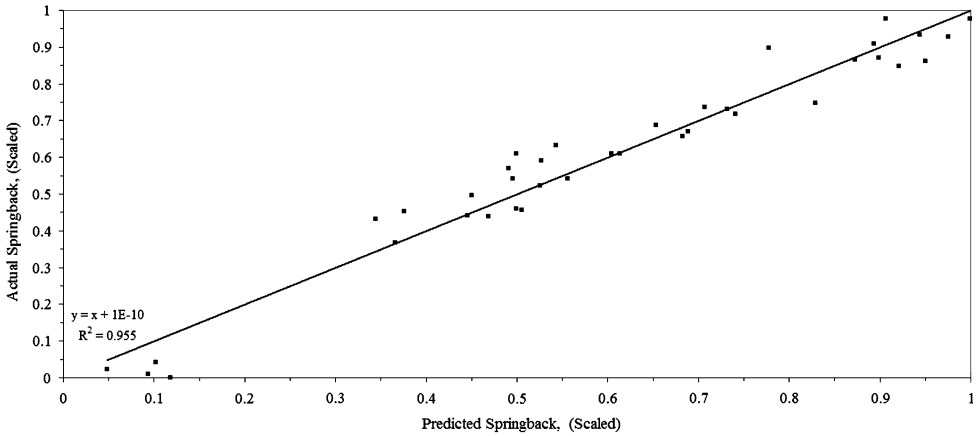

Fig. 6 Actual versus predicted springback using the CART-ANFIS numerical technique proposed by Jang et al. [17]

$$
\begin{aligned}
w_{1,i} &= 1 - \frac{1}{1+\exp[-3.2463(x_{3,i}-0.0992)]} \\
w_{2,i} &= \min\left\{\frac{1}{1+\exp[-3.2463(x_{3,i}-0.0992)]}, 1 - \frac{1}{1+\exp[-2.5120(x_{1,i}-0.4424)]}\right\} \\
w_{3,i} &= \min\left\{\frac{1}{1+\exp[-3.2463(x_{3,i}-0.0992)]}, \frac{1}{1+\exp[-2.5120(x_{1,i}-0.4424)]}\right\}
\end{aligned}
\tag{9c}
$$

Figure 6 summarises the predictive performance of this CART-ANFIS model. It performs much better than all the analytical models. The best fit line in Fig. 6 has an intercept very close to zero and a slope of unity so that this model has negligible amounts of systematic bias in predicting springback. For the analytical models about 11% of the errors made in prediction were systematic in nature. This is confirmed in Table 4 where $U_M = U_R = 0$ and in Table 2 where $U_M + U_R \approx 11\%$. The MSE of the CART-ANFIS model is also about half that of the two analytical models studies above.

This suggests that springback can be adequately modelled using a simple linear regression equation, provided that it is applied separately to appropriately chosen subsets of the data. This offers a very simple technique for analysing what is a quite complex relationship.

Right first-time manufacturing

This CART-ANFIS model can now be used to compensate for springback and so ensure right first-time manufacturing. All that is required is that a material is selected for the manufacture of the tubular shape. Once the material and its thickness are selected this predetermines the value for the yield stress and Young's Modulus. Then the bend radius

Table 4 The MSE and its decomposition for the CART-ANFIS springback model

	CART-ANFIS network
MSE	0.00322
U_M	0.00
U_R	0.00
U_D	100.00

MSE is the mean squared error as defined by Eq. 6a. U_M, U_R and U_D are % decompositions of the MSE as defined by Eq. 8b

can be chosen so as to achieve a target springback and this allowance for springback made so that the open tubular shape welds together correctly. For example, suppose material Nizec260 in Table 1 is the material chosen for the manufactured tube. It has a yield strength of around 257 MPa with Young's Modulus around 214,870 MPa (in scaled terms $x_2 = 0.756$ and $x_3 = 0.0959$). A springback compensation of say 0.82 (in scaled terms $y = 0.453$) can then be achieved through the correct selection of the bend radius. These are found simply by solving Eq. 9 under these conditions, i.e.,

$$0.453 = w_{1,i}f_{1,i}() + w_{2,i}f_{2,i}() + w_{3,i}f_{3,i}() \quad (10)$$

where the terms on the right-hand side of Eq. 10 are given by Eqs. 9b, c above with $x_{2,i} - 0.756$ and $x_{3,i} = 0.0959$.

There are a number of combinations of x_1 and x_4 that satisfy Eq. 10 and these can easily be found by hand, or for example, using Excel's Solver function. For example, $x_1 = 0.0217$ and $x_4 = 0.4852$ achieve, this level of springback. These are scaled values for x_1 and x_4, and in unscaled units this corresponds to $x_1^* = 0.694$ mm and $x_4^* = 27.871$ mm. With the bend radius and thickness set at these values the material will experience a springback of 0.82, and this can be compensated for in the bending operation to ensure right first-time manufacturing.

This type of calculation can be carried out to find the bend radii (for a given thickness) needed to achieve other degrees of springback for this material and for other materials as well.

Conclusions

This paper looked at a number of analytical models and one numerical model of springback. Using the MSE and its decomposition the predictive accuracies of a number of well-known analytical models of springback were measured. This was then compared to the predictive accuracies associated with a CART-ANFIS network. The CART-ANFIS network was found to have no systematic bias in the springback prediction made, whilst for the analytical models the systematic bias accounted for about 11% of the mean square error. The paper ended with an illustration of how the network could be used to calculate the springback for a particular material with different thicknesses that are subjected to different bend radii in the forming operation. Knowing this springback, compensation can be built into the forming operation to ensure right first-time manufacturing.

References

1. Marando RA (1999) Tubular hydroforming: the enabling technology. In: Proceedings of the international conference on hydroforming, Fellebach/Stuggart, Germany, October 12–13
2. Queener A, DeAngelis RJ (1968) Trans Am Soc Met 61:757
3. Corus introduces the Tubular Blank for the automotive industry at http://www.corusgroup.com/en/news/news/2000/2000_tubular_blank_for_automotive_industr
4. Mullan HB (2004) Formability of Corus Tubular Blanks, Doctorate Thesis, University of Wales Swansea
5. Corus celebrates first production contract for laser welded tubular blanks at http://www.corusgroup.com/en-GB/news/news/2002/2002_laser_welded_tubular_blanks_celebratio
6. Bollinger E, Jutten F (1999) Tubes for hydroforming. In: Proceedings of the international conference on hydroforming, Fellebach/Stuggart, Germany, October 12–13
7. Gardiner FJ (1957) Trans ASME 79:1
8. Marciniak Z, Duncan JL (1992) Mechanics of sheet metal forming, 1st edn. Edward Arnold, London
9. Zhang T, Hu SJ (1997) J Mater Manufact 106:458
10. Daw-Kwie L (1997) J Mater Process Technol 66(1–3):9
11. Hill R (1950) The mathematical theory of plasticity. Clarendon Press, Oxford
12. Montgomery DC (2005) Design and analysis of experiments, 2nd edn. John Wiley & Sons Inc, New York
13. Myers RH, Montgomery DC (2005) Response surface methodology: process and product optimisation using designed experiment. John Wiley & Sons Inc, New York
14. Breiman L, Friedman JH, Olshen RA, Stone CJ (1984) Classification and regression trees. Wadsworth International Group, Belmont
15. Cook RD, Weisberg S (1982) Residuals and influence in regression. Chapman & Hall, London
16. Tsoukalas LH, Uhrig RE (1997) Fuzzy and neural approaches in engineering, chapter 2. John Wiley & Sons Inc, New York
17. Jang JSR, Sun CT, Mizutani E (1997) Neuro-Fuzzy and soft computing: a computational approach to learning and machine intelligence, chapter 12. Prentice Hall, Upper Saddle River
18. Takagi T, Sugeno M (1995) IEEE Trans Syst Man Cybern 15:116
19. Theil H (1966) Applied economic forecasting. Rand McNally & Company